

Article

Temporal and Spatial Variations in Drought and Its Impact on Agriculture in China

Wen Liu ^{1,2,*} and Yuqing Zhang ³ ¹ College of Urban and Environmental Sciences, Northwest University, Xi'an 710127, China² Shaanxi Key Laboratory of Earth Surface System and Environmental Carrying Capacity, College of Urban and Environmental Sciences, Northwest University, Xi'an 710127, China³ School of Geography and Planning, Huaiyin Normal University, Huai'an 223300, China; geonuist@foxmail.com

* Correspondence: liuwen@nwu.edu.cn

Abstract: Drought, as a widespread natural calamity, leads to the most severe agricultural losses among all such disasters. Alterations in the yield of major global agricultural products are pivotal factors influencing food prices, food security, and land use decisions. China's rapidly expanding demand for sustenance will persist over the forthcoming decades, emphasizing the critical need for an accurate assessment of drought's impact on food production. Consequently, we conducted a comprehensive evaluation of the drought risk in China and its repercussions on agricultural output. Additionally, we delved into the underlying factors driving changes in yield for three primary grain crops (wheat, corn, and rice), which hold particular relevance for shaping effective strategies to mitigate future drought challenges. The findings divulge that both the number of drought months (DM) and the drought magnitude index (DMI) have displayed an upward trajectory over 60 years with a correlation coefficient of 0.96. The overall severity of meteorological drought has escalated across China, and it is particularly evident in regions such as the southwest and central parts of the Huang-Huai-Hai region, the northwestern middle region, and the Xinjiang region. Conversely, there has been some relief from drought conditions in southern China and the Yangtze River Delta. Shifts in the total grain output (TGO) during this period were compared: it underwent three stages, namely "fluctuating growth" (1961–1999), then a "sharp decline" (2000–2003), followed by "stable growth" (2004–2018). Similarly, changes in the grain planting area (GPA) experienced two stages, "continuous reduction" (1961–2003) succeeded by "stable growth" (2004–2018), while maintaining an upward trend for grain yield per unit area (GY) throughout. Furthermore, it was revealed that the drought grade serves as a significant constraint on continuous expansion within China's grain output—where the drought damage rate's influence on the TGO outweighs that from the GY. Our research outcomes play an instrumental role in deepening our comprehension regarding how drought impacts agricultural production within China while furnishing the scientific groundwork to devise efficacious policies addressing these challenges.

Keywords: meteorological drought; total grain output; grain planting area; grain yield per unit area



Citation: Liu, W.; Zhang, Y. Temporal and Spatial Variations in Drought and Its Impact on Agriculture in China.

Water **2024**, *16*, 1713. <https://doi.org/10.3390/w16121713>

Academic Editor: Thomas C. Piechota

Received: 17 May 2024

Revised: 3 June 2024

Accepted: 13 June 2024

Published: 16 June 2024



Copyright: © 2024 by the authors. Licensee MDPI, Basel, Switzerland. This article is an open access article distributed under the terms and conditions of the Creative Commons Attribution (CC BY) license (<https://creativecommons.org/licenses/by/4.0/>).

1. Introduction

Climate change has led to a continuous rise in global temperatures [1], causing an acceleration of the hydrological cycle and increasing the probability of extreme drought events [2], even in humid regions, where droughts are now occurring more frequently than ever before [2]. Over the past 20 years, the duration and frequency of droughts worldwide have increased by 29% [3], and increasingly frequent and severe drought events are undermining the achievement of sustainable development goals [4] and having a significant impact on agricultural production [5,6]. Drought events are often associated with complex emergencies involving multiple and compound disasters, such as food shortages.

In 2021, there were 15 severe drought events globally, and Asia was one of the most severely affected regions [7]. Drought-induced crop production losses exceed 30 million tons per year, making it one of the most serious meteorological and agricultural disasters threatening China's food security and social development [8,9]. Therefore, understanding the distribution features of droughts and their relationship with crop production is crucial for drought prediction, drought management, and agricultural production [10].

Different disciplines have different needs, and the definition of drought varies accordingly [11]. The International Centre for Disaster Risk Reduction (CRED) notes that drought is a long-term, gradual natural disaster that is different from short-term, sudden disasters such as floods and hurricanes. Drought usually takes a long time to form and has widespread impacts, including water shortages, declining crop yields, economic losses, and social unrest. Therefore, it is important to plan and prepare for drought in the long term, including establishing effective early warning systems, developing rational water management policies, and promoting water-saving technologies [12]. Drought is typically classified into four types based on the varying degrees of water scarcity [13]. The causes of all drought types are essentially the same; when the available water volume in different components of the hydrological cycle falls below expected levels, this leads to water scarcity [2,14–16]. The major impact of meteorological drought is reflected in crop yield reduction and groundwater depletion [11]. The impact of meteorological drought on drought propagation varies across different seasons. During the summer, meteorological drought significantly exacerbates agricultural drought, leading to an increased probability of agricultural drought occurrence as the severity of meteorological drought intensifies, consequently resulting in reduced grain yield [17]. At the same time, it is projected that global food demand will increase by 30% to 62% above the level of 2010 by 2050 [18]; therefore, in addition to improving crop varieties, the most effective and long-lasting approach is to reduce the limitation of water scarcity on crop yields through irrigation and other means [19]. In warm regions, a temperature rise will intensify the drought pressure, shorten the growing period, increase the variability of crop yields, and increase the risk of crop failure [20,21]. In cold regions, however, climate warming may extend the growing period and increase crop yields [22]. Against the backdrop of climate change, the profound effects of extreme weather and climate variability on agricultural production cannot be overstated [23]. The occurrence of meteorological drought as the initial stage in the development of other types of drought underscores its critical importance in research, contributing to addressing disaster prevention and mitigation, as well as ensuring food production in agriculture, rural areas, and for farmers [24].

Meteorological drought is a physical process that describes the water deficit at the land surface and atmospheric interface [25]. It is difficult to prevent and control the occurrence and development of such droughts, but measures for mitigation can be implemented to alleviate or halt the adverse impacts of agricultural and hydrological droughts [16]. Currently, the research on loss and damage is more focused on rapid-onset disaster events, while slower-occurring droughts receive comparatively less attention [26]. Some studies predict meteorological drought by measuring the water content in chlorophyll, using the vegetation health index, etc. [27]. The precision, efficiency, and convenience of drought indices make them a focal point in the research on drought monitoring and early warning systems, leading to extensive studies on both the suitability of existing indices and the development of new ones [28–32]. The modified Palmer drought index is believed to have better performance in meteorological drought monitoring and assessment in China [33–35]. Many studies have evaluated the suitability of different types of drought indices in China, and it has been found that the sc-PDSI is the most suitable drought index [36,37]. Some studies have explicitly stated that sc-PDSI is widely used for drought monitoring, and the characteristics of sc-PDSI are more suitable for measuring longer-term drought [34,38–40]. The extent of the impact of drought is closely related to the drought intensity grade expressed by the drought index and is also affected by the frequency and duration of drought [41,42]. There have been many studies focusing on the temporal trends and spatial

distribution of drought [43–46], drought disaster prevention and prediction [47–49], or on analyzing the impact of drought disasters on the TGO based on crop models or statistical models [50–52]. However, there has been a lack of analysis on the changes in the GY and GPA, as well as on the impact of drought on the rate of change in the TGO. Overall, the current research on the spatial and temporal distributions of drought on agricultural production is still not comprehensive. A large number of studies have shown that crop yields are affected by drought [53–55], but there is a lack of diversified crop yield indicators, and there is also a lack of analysis on the impact of different levels of drought on the rate of change in the TGO. The rate of change in the TGO reflects the sustainable development of agricultural production. How drought affects the TGO change rate and the change rate of the GY, how the TGO responds to different levels of drought, and whether the disaster rate has the same impact on the TGO and the GY need to be further strengthened.

The primary aims of this study are to (1) analyze the temporal and spatial trends in the DM and DMI to assess the evolving pattern of drought in China from 1961 to 2018; (2) elucidate the spatial distribution characteristics and temporal structural changes in the TGO and GY across all 31 provinces, municipalities, and autonomous regions in China from 1961 to 2018; (3) examine the distribution features of drought and its correlation with the rate of change in the TGO as well as the rate of change in the GY, while evaluating the impact of crop damage rate on the TGO and GY; and (4) to investigate the temporal and spatial changes in corn, rice, and wheat planting areas and their impact factors on yield. The research results are expected to deepen our understanding of the evolution of drought in China and its impact on agricultural production, thereby providing a scientific basis for weather disaster early warnings and targeted disaster prevention and reduction measures.

2. Materials and Methods

2.1. Site Description

The vast expanse of China spans multiple climatic zones, with a high frequency of drought occurrences, and the characteristics of droughts caused by climate change show obvious spatial heterogeneity. According to the “Handbook of Meteorological Geographical Classification” issued by the China Meteorological Administration [56], the land meteorological geographical division of China is divided into 10 regions (Figure 1). The division takes into account the terrain and climate types and reflects China’s different geographical features, relying on the advantage of rain and heat brought by the monsoon occurring at the same time, on the grain production pattern being “rice in the south and wheat in the north”, and on the grain crops transitioning from one crop per year or two crops in three years in the north to two crops per year in the south.

2.2. Database

This paper uses daily climate data from 1961 to 2018 (including temperature and precipitation data) from 1978 meteorological stations in China, which were sourced from <http://data.cma.cn> (accessed on 1 January 2024).

The food data for the period from 1961 to 2018 uses a spatial scale of provincial units and were sourced from the China Agricultural Statistical Data, which was accessed at <http://www.stats.gov.cn> (accessed on 1 January 2024).

2.3. Data Analysis Method

(1) Calculation of the sc-PDSI

The PDSI can be expressed as follows [57]:

$$X_i = 0.897X_{i-1} + (1/3)Z_i \quad (1)$$

In the equation, X_i and Z_i represent the PDSI and moisture anomaly index for the i -th month, respectively.

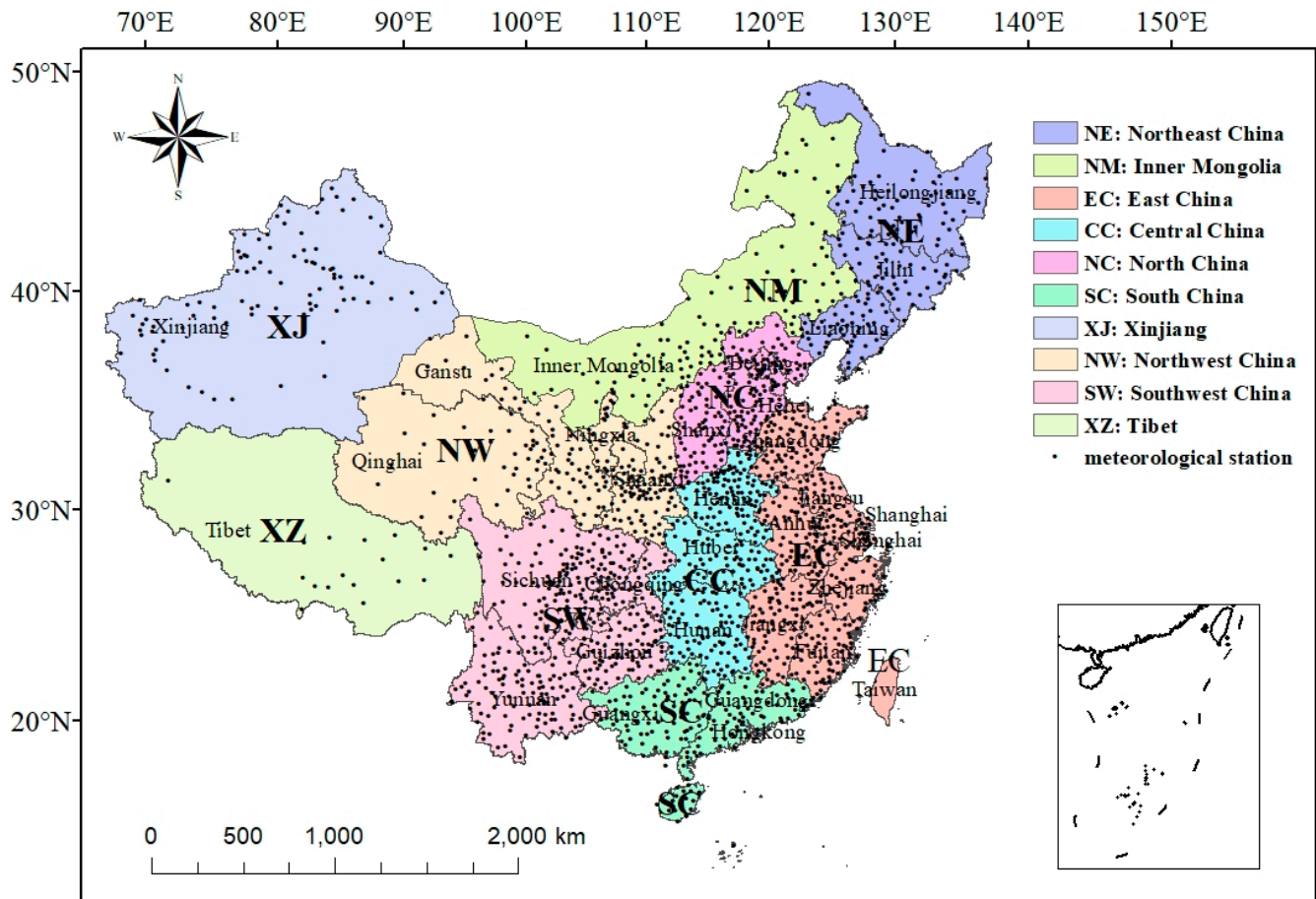


Figure 1. Study area.

In this paper, we use the self-calibrated PDSI, referred to as sc-PDSI, which can be expressed as:

$$sc - PDSI = X_i K \tag{2}$$

In this equation, K is calculated using Equations (3) and (4), where K' is a general approximate value of PDSI for the climate characteristics of a certain location [57].

$$K' = 1.5 \log_{10} \left[\left(\frac{\overline{PE} + \overline{R} + \overline{RO}}{\overline{P} + \overline{L}} + 2.80 \right) / \overline{D} \right] + 0.50 \tag{3}$$

$$K = \frac{16.84}{\sum_1^{12} \overline{DK}'} K' \tag{4}$$

In Equation (3), \overline{PE} represents the average potential evapotranspiration, \overline{R} represents the average soil moisture supply, \overline{RO} represents the average soil runoff, \overline{P} represents the average precipitation, \overline{L} represents the average soil moisture loss, and \overline{D} represents the average soil moisture deficit. Equation (4) is used to modify the K' value [57]. The drought severity levels of the sc-PDSI can be referenced against the drought classification standard established by Wells et al. [39].

(2) Drought months (DM)

The number of DM is the proportion of months with drought occurring during the study period, expressed as [58]:

$$M = \frac{n}{N} \tag{5}$$

In this formula, n represents the number of months with drought (sc-PDSI $Z \leq -1$), and N represents the total number of months.

(3) Drought magnitude index (DMI)

The DMI is used to evaluate the severity of drought in the study area. When the drought reaches the cumulative value of 1, which is the sc-PDSI value, the higher the value, the more severe the drought, and the lower the value, the lighter the drought. The calculation formula is as follows [58]:

$$MI = \sum_{n=1}^n |Z_i - S| \quad (6)$$

In this formula, Z_i represents the sc-PDSI value at the i -th grid point ($i = 1, 2, 3, \dots, k$), and S is the drought index threshold, which is set to -1 in this paper.

(4) Linear trend coefficient

When analyzing the frequency of droughts and changes in grain yields, the linear trend rates are calculated using linear regression equations, which are as follows [34]:

$$X_i = a + bt_i, i = 1, 2, 3, \dots, n \quad (7)$$

In this formula, X_i represents a factor, t represents the corresponding time for X_i , and b represents the linear trend.

(5) Rate of change

$$\Delta Y_i = \frac{Y_i - Y_{i-1}}{Y_{i-1}} \times 100\% \quad (8)$$

In the formula, ΔY_i represents the rate of increase or decrease in the TGO or GY; i represents a specific year, and $i-1$ represents the year prior to the year i ; Y_i represents the TGO or GY in the year i ($i = 1, 2, 3, \dots, k$); and Y_{i-1} represents the TGO or GY in the previous year $i-1$.

3. Results

3.1. Drought Characteristics

From the spatial distribution of the average number of DM from 1961 to 2018 (Figure 2a), it can be seen that the duration of droughts is mostly between 4–6 months. By calculating the trend of DM at each site using linear trend fitting (Figure 2b), it was found that the sites with a change trend in DM exceeding 50% were concentrated in the western NE, eastern NM, NC, central NW, northern CC, and SW regions. The area where the DM had increased is in the region connecting the northeast and southwest and is roughly around the Hu's line. The change rate of DM in the XJ, southern CC, central EC, eastern NE, and northwestern SW regions was negative, indicating that the duration of droughts in their respective regions was decreasing.

The average DMI (Figure 2c) shows that the drought level at most sites is at level 6 or above, which is closely related to the longer duration of drought at most sites. The trend for the change in the DMI (Figure 2d) has a similar spatial distribution to the trend for the observed change in the duration of drought (Figure 2b), and the sites with a change rate in the DMI exceeding 100% are mostly concentrated near the Hu's line. The NE, NC, CC, NW Midwest, and SW regions have the largest change rates, indicating that these areas have a gradually increasing DMI and increasing drought, which is consistent with the analysis earlier. The areas where the DMI shows an increasing trend also show an increasing trend in the number of DM. The XJ, the southern part of the CC, the central and southern part of the EC, the eastern part of the NE, and the northwestern part of the SW regions have negative change rates in the DM, indicating that the DMI in these areas has decreased and the drought situation has improved.

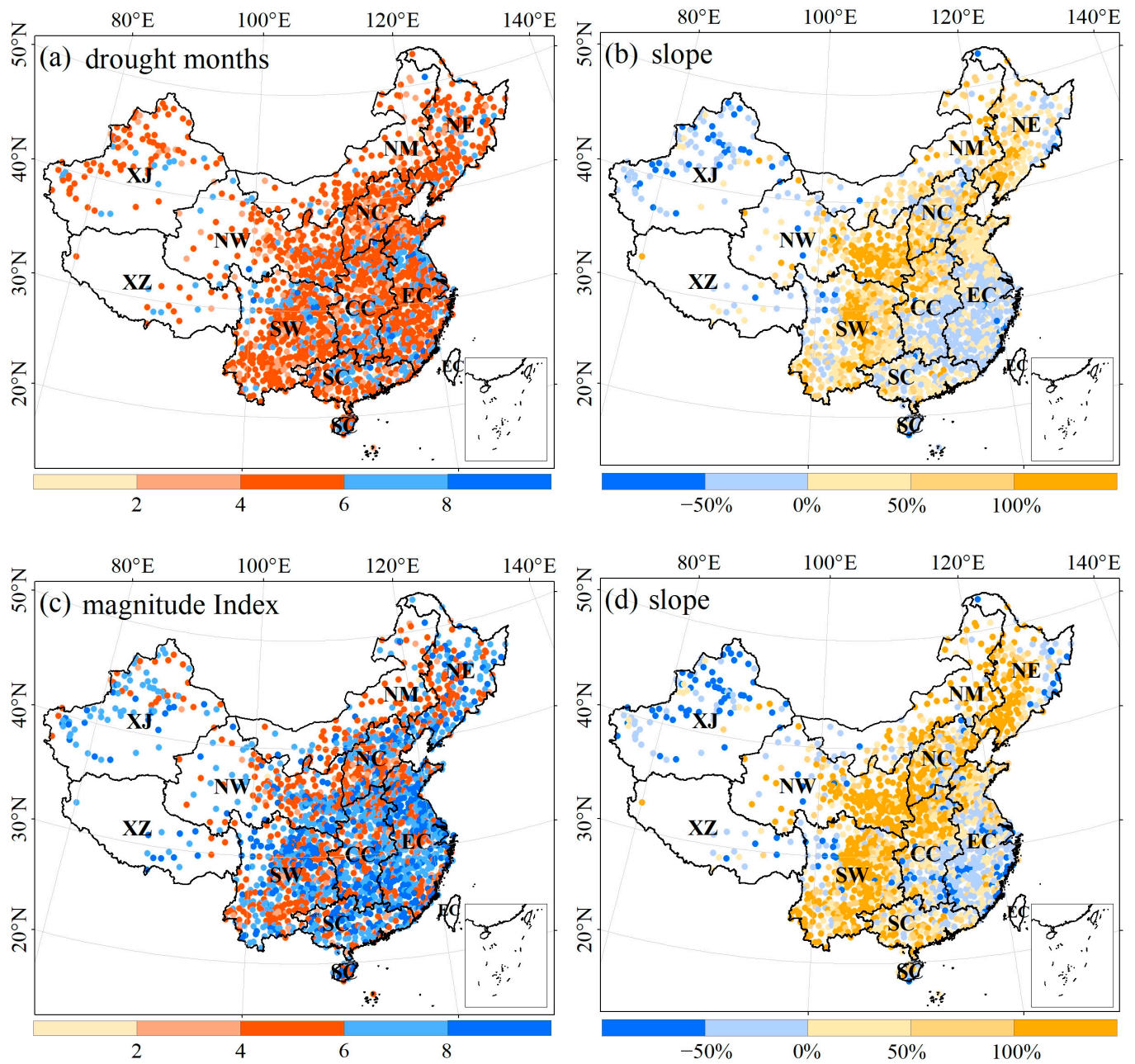


Figure 2. Distribution of the drought months (a), trend in drought months (b), drought magnitude index (c), and trend in the drought magnitude index (d) in China from 1961 to 2018.

The interdecadal variations in the drought duration and intensity are highly consistent, showing an “up–up–down–up–up–down” pattern. Although the drought duration and intensity have shown a downward trend in the past 10 years, the DM and DMI have shown an upward trend on a 60-year scale (Figure 3). The correlation between drought duration and intensity is extremely high, with the correlation between the annual average DM and DMI reaching 0.92 (Figure 4a) and the correlation between annual DM and DMI reaching 0.96 (Figure 4b).

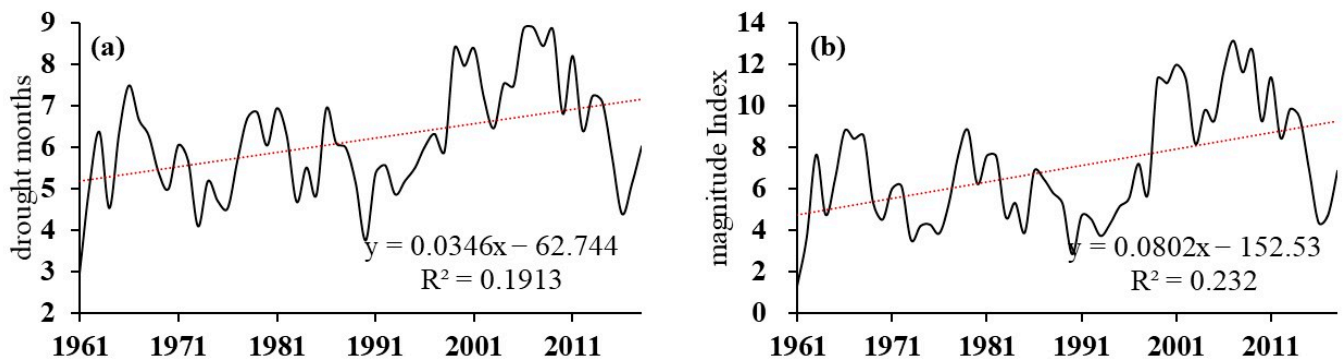


Figure 3. Time distribution characteristics of the annual average drought months (a) and drought magnitude index (b) from 1961 to 2018.

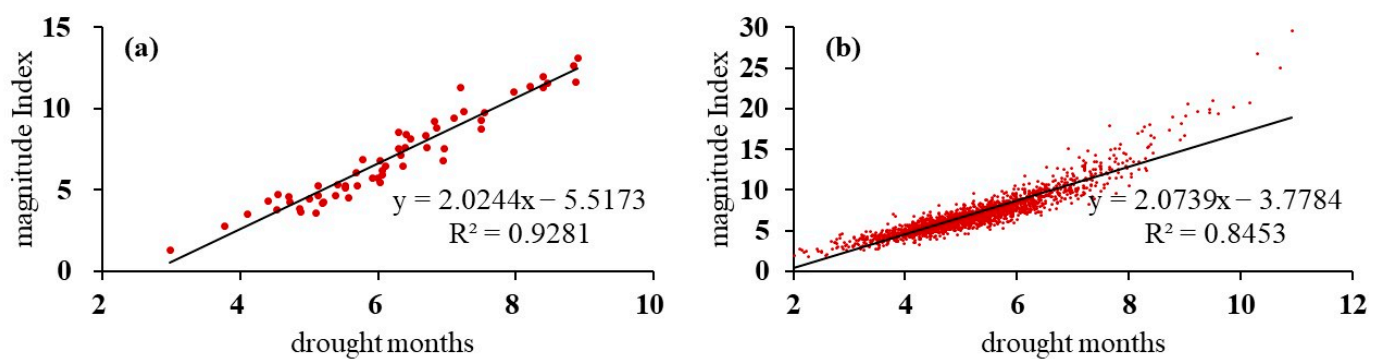


Figure 4. Correlation between the drought months and drought magnitude index at different scales: (a) site scale; (b) site average.

3.2. Characteristics of the Drought Trend

From 1961 to 2018, the sc-PDSI experienced a rate of change of $-0.01/\text{decade}$, signifying a marginal overall escalation in the severity of meteorological drought across China (Figure 5). Notable amplifications in drought patterns were evident in the SW, CC, NC, and NW's middle and eastern regions, with the sc-PDSI index exhibiting a rate of change of less than $0/\text{decade}$ (Figure 5a) and demonstrating statistical significance through tests ($p < 0.05$ or $p < 0.01$) (Figure 5b). Provinces (cities, autonomous regions) manifesting substantial drought trends encompass Liaoning, Hebei, Shandong, Shanxi, Henan, Shaanxi, Ningxia, southern Gansu, southeastern Sichuan, Chongqing, Guizhou, and Yunnan. The trend in drought in the Xinjiang, Sichuan, and Jiangnan regions is greater than zero, indicating that there has been some relief from drought or even a trend toward moisture; moreover, the moisture trend in Xinjiang passed significance tests.

3.3. Characteristics of Changes in Grain Yields

The TGO of China is roughly divided by the Hu's line, showing a pattern of more in the southeast and less in the northwest (Figure 6a). The annual average grain output of Henan, Sichuan, Shandong, Heilongjiang, Jiangsu, Hunan, Anhui, and Hebei is all over 2000×10^4 t. The provinces with the fastest growing grain output are Heilongjiang and Henan, with an increase of over 1000×10^3 t/decade, and thanks to the abundant land resources and the vigorous development of agriculture, the grain output has been continuously increasing (Figure 6b). The economically developed provinces of Zhejiang, Guangdong, Beijing, Shanghai, and Chongqing show a downward trend in their TGO. The main grain-producing areas of Heilongjiang, Inner Mongolia, Jilin, Shandong, Henan, and Hebei are affected by drought to a greater extent; if these areas frequently suffer from drought, it may cause food security problems and undermine social stability.

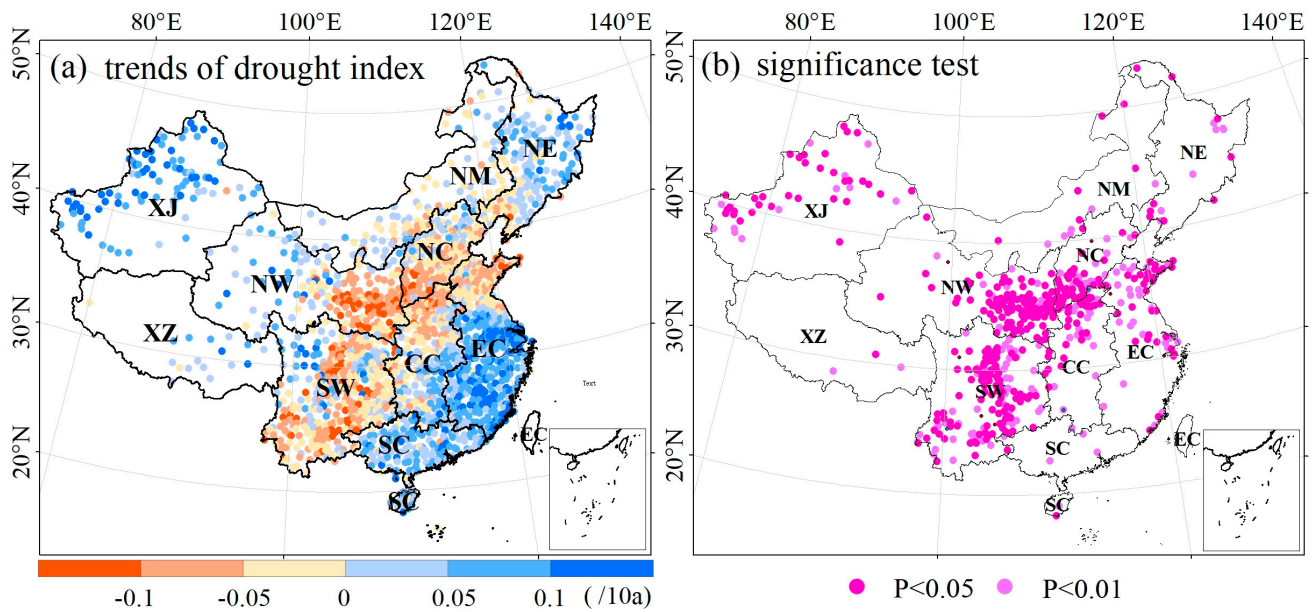


Figure 5. The trend and significance test for the sc-PDSI from 1961 to 2018.

The distribution of the GPA and TGO is highly consistent, generally showing an east–west imbalance (Figure 6c). The provinces with a GPA exceeding 8000×10^3 ha are Henan, Heilongjiang, Sichuan, and Shandong. The province with the highest GPA growth rate exceeding 1000×10^3 ha/decade is Heilongjiang, thanks to the government’s strong support for agricultural development (Figure 6d). Due to the rapid urbanization process, most provinces in the country have seen a decline in their GPA.

Provinces with grain yields exceeding 4.2 t/ha are mainly concentrated in economically developed regions such as the Yangtze River Delta and the Beijing–Tianjin–Hebei region, largely because these areas have lower GPAs (Figure 6e). Excluding this factor, the high yields and lower planting areas in Hunan and Jilin make their grain yields relatively high. Looking at the trend in grain yield changes, the change rate of grain yield in all the regions of the country is increasing, with a general pattern of being low in the east and high in the west (Figure 6f). The change rate of grain yield in Heilongjiang is lower than 0.6 t/decade, while that in Tibet is higher than 1.2 t/decade.

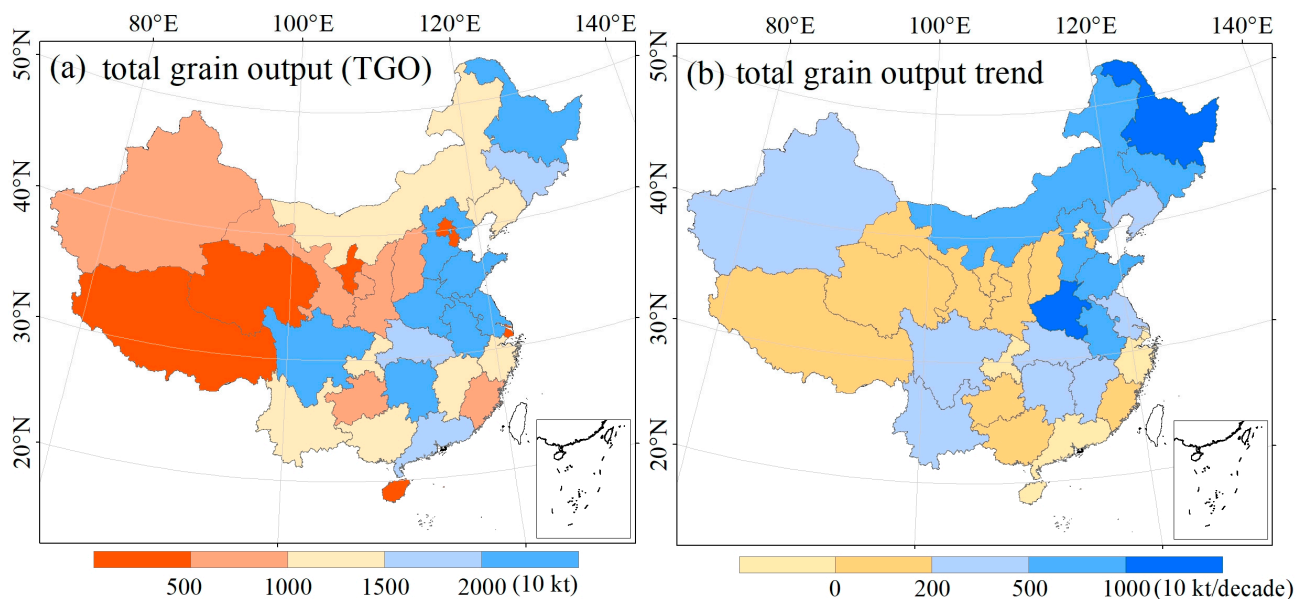


Figure 6. Cont.

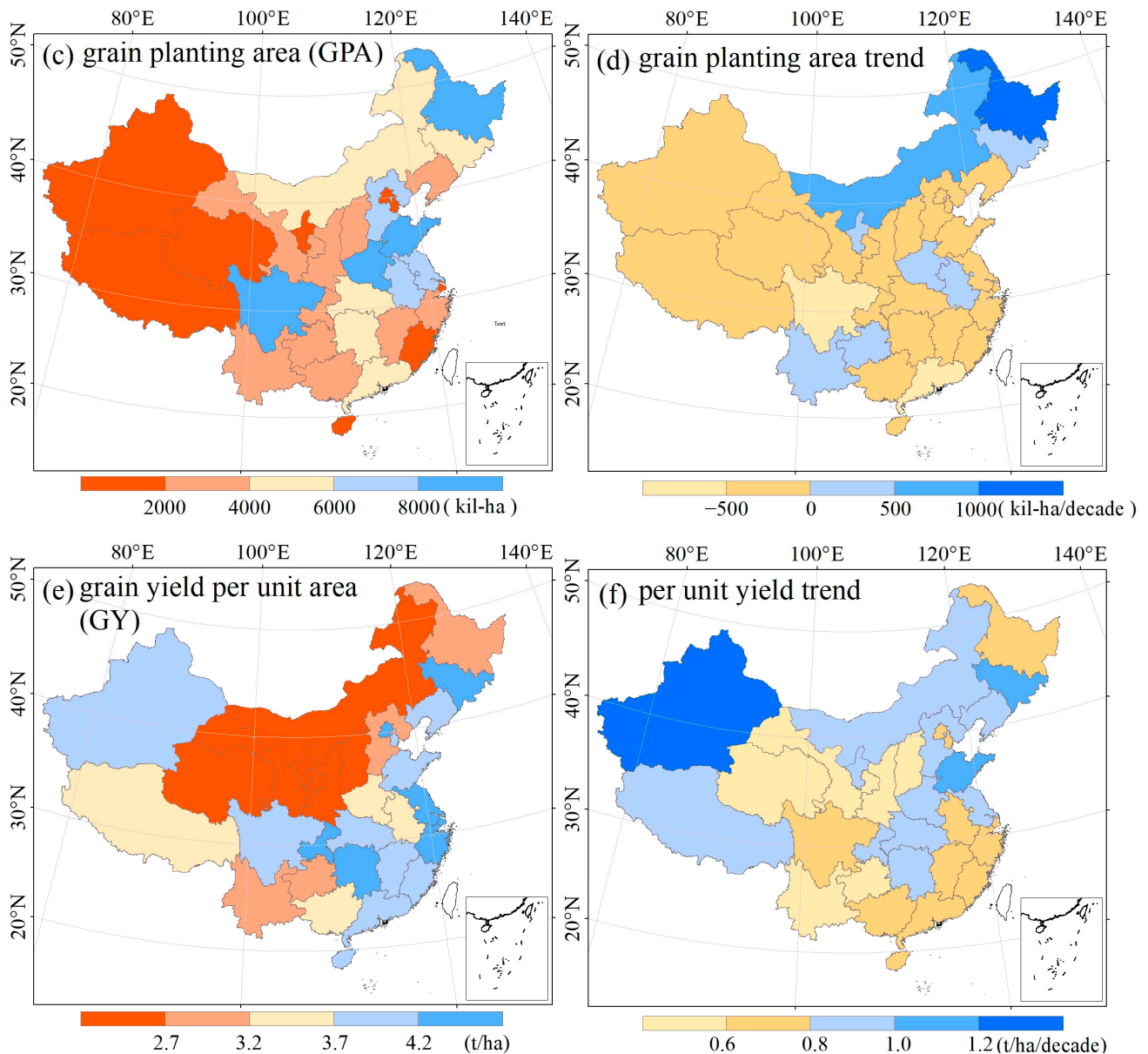


Figure 6. Spatial distribution and trends of the total grain output, grain planting area, and grain yield per unit area.

The changes in TGO can be divided into three stages: fluctuating growth from 1961 to 1998, a sharp decrease from 1998 to 2003, and stable growth from 2003 to 2018, with a rate of change of 0.97×10^8 t/decade, -1.59×10^8 t/decade, and 1.617×10^8 t/decade, respectively. The changes in GPA can be divided into two stages: a decline from 1961 to 2002 and continuous growth from 2002 to 2018, with a rate of change of -0.38×10^8 ha/decade and 0.13×10^8 ha/decade, respectively. The trend in the GY is relatively consistent, showing an upward trend, with a rate of change of 0.78 t/ha. As shown in Figure 7a–c, the TGO and GPA have been changing constantly, while the GY has always maintained a stable upward trend, indicating that grain yield is also affected by other factors, such as drought and agricultural technology level. To eliminate the influence of other factors, further analysis of the rate of change in grain unit area yield over a long time sequence shows that the rate of change in the GY is decreasing at a rate of -0.1064% /decade (Figure 7d).

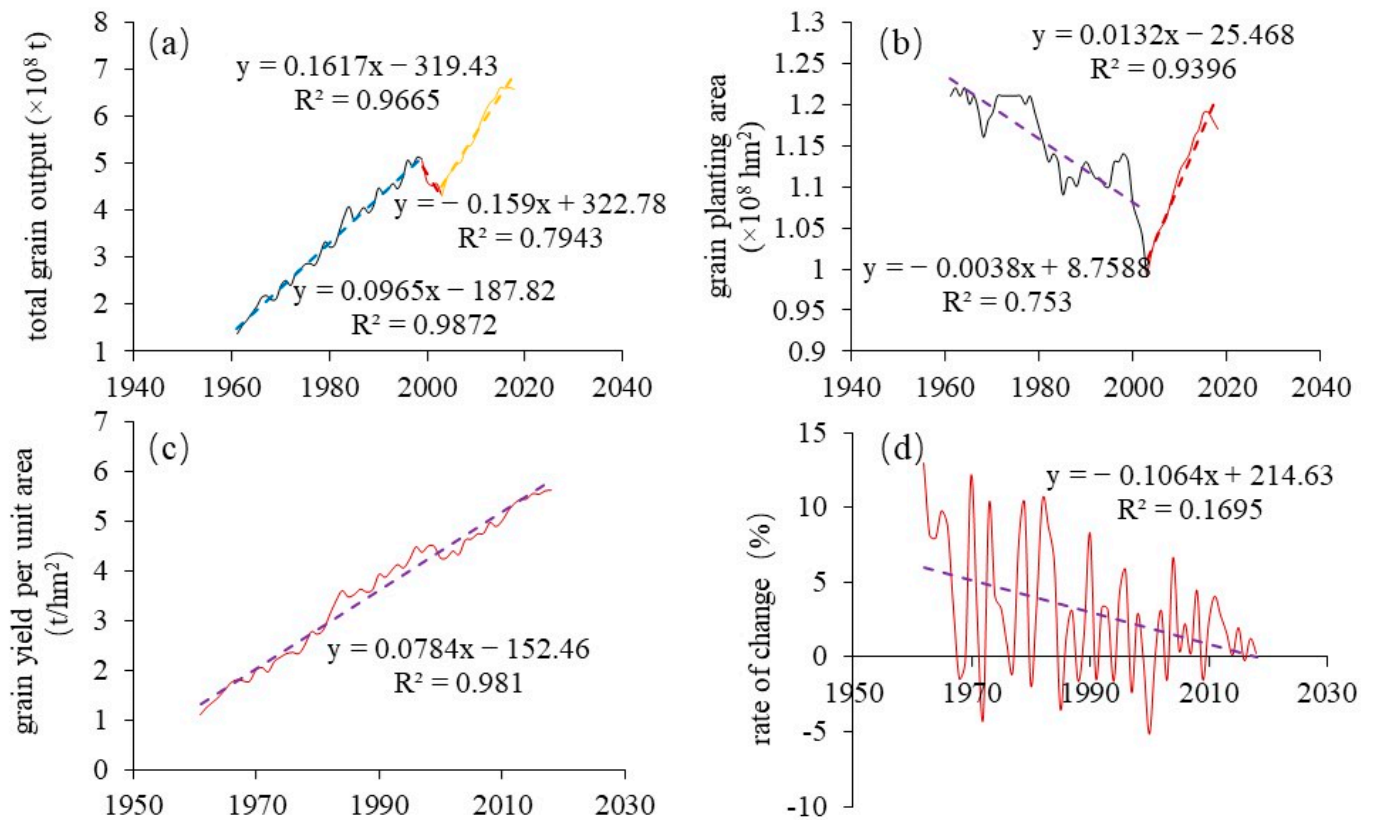


Figure 7. Total grain output, grain planting area, and grain yield per unit area and the change rate of grain yield per unit area from 1961 to 2018.

3.4. The Impact of Drought on Crop Yields

The annual variation rate of the TGO shows an upward trend with fluctuations, and it is negatively correlated with the drought index level (Figure 8a). In years with high drought index levels, the annual variation rate of TGO is low, and the valley of the drought index curve corresponds to the peak of the annual variation rate of TGO. As the drought index fluctuates upwards with a growth rate of 0.80/decade, the annual variation rate of TGO fluctuates downwards at a rate of $-0.89/\text{decade}$ (Figure 8a). The change in GY is less constrained by climate factors and is more comparable, being unaffected by time and spatial geographical factors, and it represents the difference in TGO between the two periods. If the result is positive, it means an increase in grain yield, and if it is negative, it means a decrease. It can be seen that the sensitivity of the GY to drought is higher, with a decline rate of $-1.064/\text{decade}$ (Figure 8b). This shows that the drought grade is an important factor restricting the continuous growth of China's grain yield.

The fluctuations in the disaster incidence rate and the fluctuations in the rate of change in the TGO also show a “peak to trough” relationship, but because the affected area, no matter how large or small, always directly affects the change in the rate of change in TGO, the trend of the change is consistent, showing a downward trend (Figure 8c). Similarly, the fluctuations in the disaster incidence rate and the rate of change in the TGO also show the same downward trend, and the “peak to trough” relationship is even more pronounced (Figure 8d). This shows that when drought disasters affect agricultural production, the growth rate of the TGO will be affected.

To further illustrate the impact of crop drought on the TGO, an analysis was conducted on the relationship between the disaster incidence rate and the TGO and GY. With the continuous improvement of agricultural disaster prevention and reduction levels, the disaster incidence rate has been declining at a rate of 1.31% per decade. The decline in the disaster incidence rate has led to an upward trend in TGO, with an increase rate of $0.85 \times 10^5 \text{ kt/decade}$ (Figure 9a). The TGO and disaster rate show a significant negative

correlation, with a correlation coefficient of 0.65. As the disaster rate decreases, the GY also increases significantly, growing by 0.78 t/ha/decade (Figure 9b). The correlation coefficient between GY and the disaster rate is 0.6, indicating that the impact of the disaster rate on TGO is greater than that of the GY.

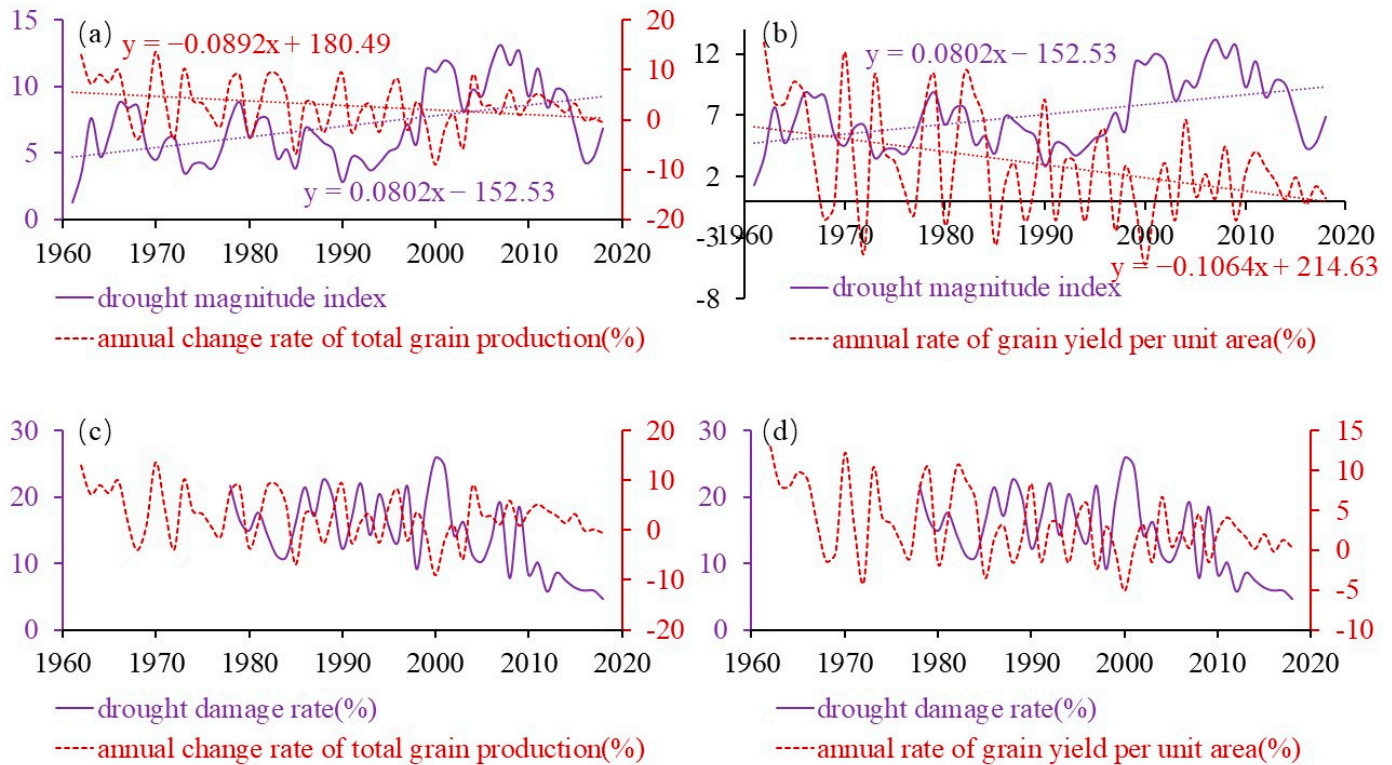


Figure 8. Comparison of the rate of change in the drought magnitude index (1961–2018) and disaster incidence rate with the rate of change in the total grain output and grain yield per unit area.

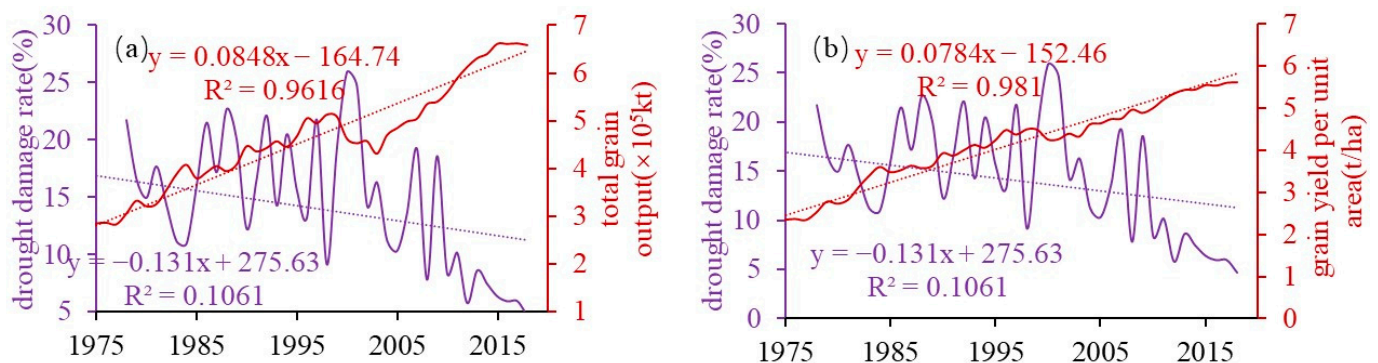


Figure 9. The trends in the disaster incidence rate and total grain output (a) and grain yield per unit area (b).

4. Discussion

This study analyzed the correlation between drought and grain yield, concluding that drought constitutes a significant meteorological threat to China’s food security. Despite the escalating impact of other disasters on agricultural production, drought remains the primary concern affecting China’s agricultural output [59]. The predominant crops in China include corn, rice, and wheat, with rice predominantly cultivated in the southern regions and wheat and corn serving as the main staples in northern China [60]. Drought exerts an influence on the yield of these three major food crops; however, their respective impact mechanisms are not uniform.

4.1. Mechanisms of Corn Yield Impact

Corn is an important crop for dry land, being mainly grown in semi-humid and semi-arid areas [61]. It is widely distributed in China and mainly concentrated in the NE, NW, and SW regions (Figure 10a,b), forming a roughly elongated corn cultivation belt from the NE to the SW, accounting for about 65% of the national corn output. The provinces with the largest planting areas are Shandong, Jilin, Hebei, Heilongjiang, Liaoning, Henan, and Sichuan. Between 2000 and 2018, the majority of the new corn planting areas were concentrated in the NE and NW, which had abundant sunlight and soil conditions (Figure 10c). During this period, China's corn output generally increased. However, the unit area yield of corn in Shanghai, Hubei, and Guizhou showed a downward trend, which may be due to the drought trend in the EC, CC, and SW regions during this period, affecting the corn output. The climate in NW is suitable for corn growth, and the corn yield has been steadily increasing. In the SW and CC regions, there are risks of local flooding and waterlogging, and there is a risk of high temperature and drought in the Sichuan Basin and the lower reaches of the Yangtze River. Sudden water and drought disasters and high temperatures and drought are not conducive to an increase in corn output. Related studies have indicated that drought prevention in corn-growing areas is very important [62,63]. The NC region has a wide area of corn cultivation due to its favorable precipitation, soil, topography, and good policy orientation, accounting for over 26% of the national corn planting area and producing about 29% of China's total corn output [64]. Recent research indicates a significant warming trend in the global climate since 2000, resulting in substantial improvements in heat conditions within the northeastern region located in the subarctic zone. This has led to a notable decrease in the probability of frost damage. With the amelioration of heat conditions, the primary factor influencing spring corn production has shifted from temperature to moisture levels. As a result, drought currently represents the foremost natural hazard to spring corn yields. However, certain studies have suggested that average annual precipitation does not exert a significant impact on corn harvests. The key climatic factor affecting corn yields remains minimum temperatures, and it is expected that further climate change will enhance corn production in the northeastern region [65]. In addition to the impact of climatic factors, returning corn straw to the fields also has a promoting effect on corn yield in the NC region [66]. The NC Plain, similar to Northeast China, is a highly productive region for corn in China [67]. However, the issue of drought in the North China region is more pronounced, and further research has confirmed that drought stress is the primary limiting factor for corn yield [68]. Based on a quantitative analysis, it has been indicated that under moderate drought, severe drought, and extreme drought conditions, corn yields would decrease by 4.91%, 10.44%, and 7.34%, respectively. The intensification of drought conditions has amplified the variability in corn yield [69], and no matter which drought index is used, the conclusion is that drought will affect corn yield [70–72].

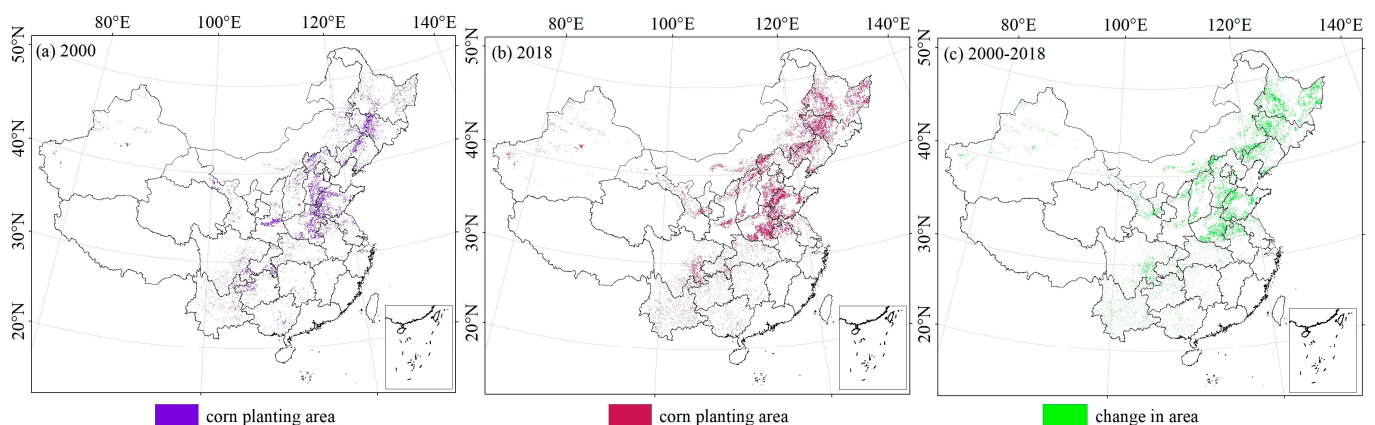


Figure 10. Spatial changes in the corn planting area from 2000 to 2018.

4.2. Mechanisms of Rice Yield Impact

Rice is concentrated in planting areas south of the Qinling–Huaihe Line, and there is scattered distribution in some water source areas in the NW and NC regions (Figure 11). Rice salt production is affected by both alkali soil and drought stress, and studies have shown that drought will reduce the rice growing period and cause a decrease in rice yield. The combined stress of saline–alkaline soil and drought leads to a more significant decrease in yield, mainly due to insufficient water resources and imperfect irrigation facilities [73]. Drought is one of the non-biological constraints on rice production [74], and current studies have found that rice exhibits leaf curling to reduce the excessive water loss caused by a water deficit, thus adapting to drought and other unfavorable environmental conditions [75]. The response of rice yield to drought is most pronounced on a 4-month time scale in autumn, with vulnerability manifested as decreased yield. Rice-growing areas are typically concentrated in humid regions with abundant water and heat, but limited sunlight hours result in a longer response time to drought [76]. Rice is a pivotal food crop, particularly for developing countries, providing sustenance for the majority of the global population. However, approximately 45% of rice-growing areas worldwide are affected by drought stress, leading to significant reductions in yields due to water scarcity. Therefore, the exploration and development of drought-resistant rice varieties represent an effective approach to addressing this challenge [77].

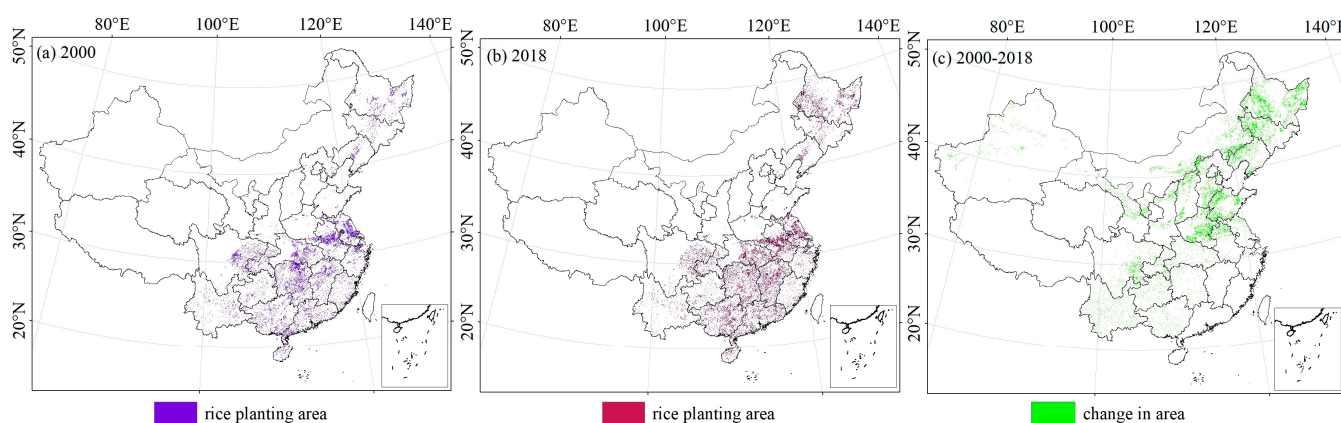


Figure 11. Spatial changes in the rice planting area from 2000 to 2018.

4.3. Mechanisms of Impact on Wheat Yield

Wheat, as a prevalent cereal crop, exhibits sensitivity to temperature factors in its growth and production. Against the backdrop of climate warming, there are anticipated changes in the duration of wheat's maturation and growing periods, which ultimately impact the grain yield [78]. The main wheat production areas in China are mainly concentrated in the NC, NW, and NC regions, and the increase in wheat planting areas from 2000 to 2018 was mainly distributed in the NC Plain (Figure 12). A study conducted on the winter and spring wheat yields of the northern provinces from 1979 to 2017 found that drought had a greater impact on crop yields than high temperatures, and pointed out that irrigation could offset the effects of high temperatures and drought on yields to some extent [60]. However, most wheat-growing areas are rain-fed agriculture, and non-irrigated areas have little impact on wheat yields [79]. With climate warming, any increase in temperature below the optimal temperature in the northern cold regions is beneficial to the improvement of wheat yield [80], but warming and drought have offset the benefits of CO₂ increases on wheat yield in the past 60 years [79]. Winter wheat in the NW region is affected by spring, summer, and winter droughts, seriously threatening its yield [81]. After 2000, the decline and fluctuation in wheat yield in the central Gansu Province of the NW region decreased significantly, and the frequency of major disasters also decreased significantly. The major disaster-prone areas shifted from the south to the

north in terms of spatial position [82]. Therefore, separating the long-term specificity and spatial specificity of drought effects on winter wheat yield can better help explain yield losses [83]. For nearly 60 years, winter wheat in North China has suffered from severe drought during the growing season, especially during the jointing and heading stages, with an average annual deficit of 350 mm of water, which has had a significant impact on its yield [84]. The drivers of drought encompass both climate change and human activities. In the NC Plain region, the contribution of climate change to agricultural drought outweighs that of human activities. Long-term droughts induced by climate change can impact the net primary productivity of winter wheat, while simultaneously, human activities also exert a significant influence on its net primary productivity [85]. Elevated temperatures, prolonged drought, and ozone exposure can all lead to significant reductions in wheat yields. However, there has been a continuous increase in O₃ concentrations, and studies indicate that current O₃ levels would result in an 8–9% decrease in global wheat production compared with pre-industrial levels [86].

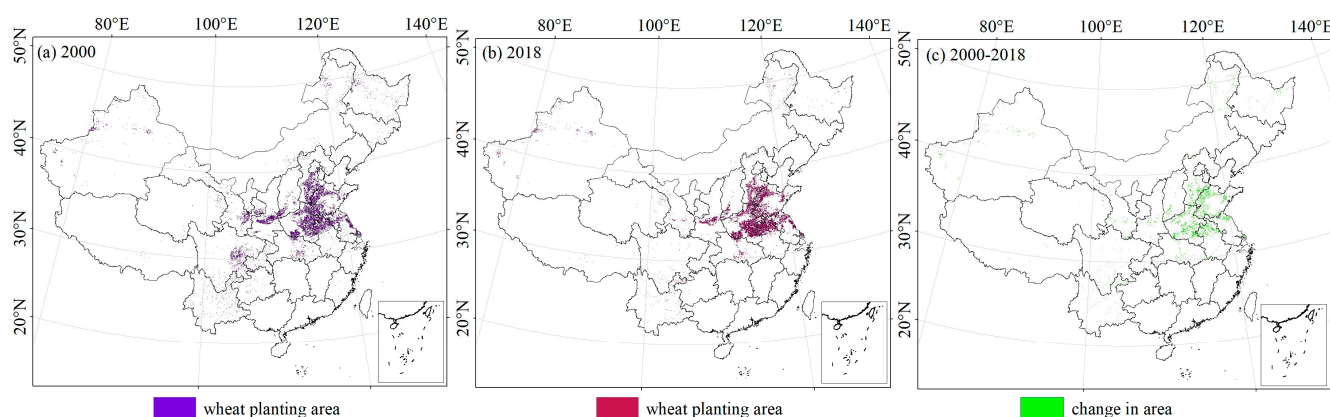


Figure 12. Spatial change in the wheat planting area from 2000 to 2018.

5. Conclusions

The number of DM and the DMI have both shown an upward trend over the 60 years, with a high correlation (0.96) on an annual scale. The sc-PDSI has shown a decreasing trend of $-0.01/\text{decade}$, suggesting an overall increase in meteorological drought severity across China. Notably significant increases in drought trends were observed along the Hu's line, which traverses the SW region through to the central, NE, and NC regions. In contrast to changes in the TGO during this period—which experienced “fluctuating growth” (1961–1999), a “sharp decline” (2000–2003), and “stable growth” (2004–2018)—the GPA underwent continuous sharp declines from 1961 to 2003 followed by stable continuous growth from 2004 to 2018. Conversely, GY has consistently increased. Furthermore, there is a negative correlation between the annual variation rate of TGO and the DMI, while TGO is significantly negatively correlated with the disaster rate. These findings suggest that drought severity plays a crucial role in constraining sustained growth of China's grain yield; additionally, drought damage rate exerts greater influence on the TGO than on the GY.

The occurrence and development of drought have a propagation process, and the agricultural adaptation to drought is also the result of multiple factors, including natural environmental factors and human factors. However, this study only analyzed the impact of meteorological drought on agriculture. As the drought propagation deepens, the impact mechanism of drought on agriculture will be different. For example, the impact process of sustained mild drought and sudden severe drought on agriculture will be different. Additionally, drought is closely related to other natural disasters such as wildfires and water shortages. In our future work, we will refine the process of drought propagation, delve deeper into the impact of different drought propagation and different drought patterns on agricultural production, and further explore the factors that influence drought.

Author Contributions: Conceptualization, writing, W.L.; Data collection, Y.Z. All authors have read and agreed to the published version of the manuscript.

Funding: This research was funded by the National Natural Science Foundation of China (Grant No. 41901110).

Data Availability Statement: The data acquisition method has been explained in the article.

Conflicts of Interest: The authors declare no conflicts of interest.

References

1. IPCC. *Climate Change 2013: The Physical Science Basis. Contribution of Working Group I to the Fifth Assessment Report of the Intergovernmental Panel on Climate Change*; Cambridge University Press: Cambridge, UK; New York, NY, USA, 2013; 1535p.
2. Mishra, A.K.; Singh, V.P. A review of drought concepts. *J. Hydrol.* **2010**, *391*, 202–216. [[CrossRef](#)]
3. Yin, G.; He, W.; Liu, W.; Liu, X.; Xia, Y.; Zhang, H. Drought stress and its characteristics in China from 2001 to 2020 considering vegetation response and drought creep effect. *J. Hydrol. Reg. Stud.* **2024**, *53*, 101763. [[CrossRef](#)]
4. Zhang, X.; Chen, N.; Sheng, H.; Ip, C.; Yang, L.; Chen, Y.; Sang, Z.; Tadesse, T.; Lim, T.P.Y.; Rajabifard, A.; et al. Urban drought challenge to 2030 sustainable development goals. *Sci. Total Environ.* **2019**, *693*, 133536. [[CrossRef](#)] [[PubMed](#)]
5. Zhang, Q.; Li, J.; Singh, V.P.; Xiao, M. Spatio-temporal relations between temperature and precipitation regimes: Implications for temperature-induced changes in the hydrological cycle. *Glob. Planet. Change* **2013**, *111*, 57–76. [[CrossRef](#)]
6. David, B.; Lobell, J.M.D.; Di Tommaso, S. Changes in the drought sensitivity of US maize yields. *Nat. Food* **2020**, *1*, 729–735.
7. CRED. *2021 Disasters in Numbers*; CRED: Brussels, Belgium, 2022.
8. Zhai, J.; Huang, J.; Su, B.; Cao, L.; Wang, Y.; Jiang, T.; Fischer, T. Intensity–area–duration analysis of droughts in China 1960–2013. *Clim. Dyn.* **2016**, *48*, 151–168. [[CrossRef](#)]
9. Zhang, Q.; Yao, Y.; Li, Y.; Huang, J.; Ma, Z.; Wang, Z.; Ying, W.; Yu, Z. Progress and prospect on the study of causes and variation regularity of droughts in China. *Acta Meteorol. Sin.* **2020**, *78*, 500–521. [[CrossRef](#)]
10. He, B.; Lü, A.; Wu, J.; Zhao, L.; Liu, M. Drought hazard assessment and spatial characteristics analysis in China. *J. Geogr. Sci.* **2011**, *21*, 235–249. [[CrossRef](#)]
11. Mukherjee, S.; Mishra, A.; Trenberth, K.E. Climate Change and Drought: A Perspective on Drought Indices. *Curr. Clim. Change Rep.* **2018**, *4*, 145–163. [[CrossRef](#)]
12. Wilhite, D.A. *Chapter 1 Drought as a Natural Hazard Concepts and Definitions. Drought a Global Assessment; Drought Mitigation Center Faculty: Lincoln, NE, USA, 2000.*
13. Liu, Y.; Shan, F.; Yue, H.; Wang, X.; Fan, Y. Global analysis of the correlation and propagation among meteorological, agricultural, surface water, and groundwater droughts. *J. Environ. Manag.* **2023**, *333*, 117460. [[CrossRef](#)]
14. Li, J.; Guo, Y.; Wang, Y.; Lu, S.; Chen, X. Drought Propagation Patterns under Naturalized Condition Using Daily Hydrometeorological Data. *Adv. Meteorol.* **2018**, *2018*, 2469156. [[CrossRef](#)]
15. Li, J.; Wang, Z.; Wu, X.; Xu, C.; Guo, S.; Chen, X.; Zhang, Z. Robust Meteorological Drought Prediction Using Antecedent SST Fluctuations and Machine Learning. *Water Resour. Res.* **2021**, *57*, e2020WR029413. [[CrossRef](#)]
16. Barker, L.J.; Hannaford, J.; Chiveron, A.; Svensson, C. From meteorological to hydrological drought using standardized indicators. *Hydrol. Earth Syst. Sci. Discuss.* **2015**, *12*, 12827–12875.
17. Xu, Y.; Zhang, X.; Hao, Z.; Singh, V.P.; Hao, F. Characterization of agricultural drought propagation over China based on bivariate probabilistic quantification. *J. Hydrol.* **2021**, *598*, 126194. [[CrossRef](#)]
18. van Dijk, M.; Morley, T.; Rau, M.L.; Saghai, Y. A meta-analysis of projected global food demand and population at risk of hunger for the period 2010–2050. *Nat. Food* **2021**, *2*, 494–501. [[CrossRef](#)] [[PubMed](#)]
19. van Ittersum, M.K.; Cassman, K.G.; Grassini, P.; Wolf, J.; Tittone, P.; Hochman, Z. Yield gap analysis with local to global relevance—A review. *Field Crops Res.* **2013**, *143*, 4–17. [[CrossRef](#)]
20. Foley, J.A.; Ramankutty, N.; Brauman, K.A.; Cassidy, E.S.; Gerber, J.S.; Johnston, M.; Mueller, N.D.; O’Connell, C.; Ray, D.K.; West, P.C.; et al. Solutions for a cultivated planet. *Nature* **2011**, *478*, 337–342. [[CrossRef](#)] [[PubMed](#)]
21. Lobell, D.B.; Schlenker, W.; Costa-Roberts, J. Climate Trends and Global Crop Production Since 1980. *Science* **2011**, *333*, 616–620. [[CrossRef](#)] [[PubMed](#)]
22. Webber, H.; Ewert, F.; Olesen, J.E.; Müller, C.; Fronzek, S.; Ruane, A.C.; Bourgault, M.; Martre, P.; Ababaei, B.; Bindi, M.; et al. Diverging importance of drought stress for maize and winter wheat in Europe. *Nat. Commun.* **2018**, *9*, 4249. [[CrossRef](#)]
23. Ceglar, A.; Toreti, A.; Lecerf, R.; Van der Velde, M.; Dentener, F. Impact of meteorological drivers on regional inter-annual crop yield variability in France. *Agric. For. Meteorol.* **2016**, *216*, 58–67. [[CrossRef](#)]
24. Sun, H.; Sun, X.; Chen, J.; Deng, X.; Yang, Y.; Qin, H.; Chen, F.; Zhang, W. Different types of meteorological drought and their impact on agriculture in Central China. *J. Hydrol.* **2023**, *627*, 130423. [[CrossRef](#)]
25. Lloyd-Hughes, B. The impracticality of a universal drought definition. *Theor. Appl. Clim.* **2013**, *117*, 607–611. [[CrossRef](#)]
26. Singh, C.; Jain, G.; Sukhwani, V.; Shaw, R. Losses and damages associated with slow-onset events: Urban drought and water insecurity in Asia. *Curr. Opin. Environ. Sustain.* **2021**, *50*, 72–86. [[CrossRef](#)]

27. Dong, X.; Zhou, Y.; Liang, J.; Zou, D.; Wu, J.; Wang, J. Assessment of Spatiotemporal Patterns and the Effect of the Relationship between Meteorological Drought and Vegetation Dynamics in the Yangtze River Basin Based on Remotely Sensed Data. *Remote Sens.* **2023**, *15*, 3641. [[CrossRef](#)]
28. Cheng, Y.; Zhang, K.; Chao, L.; Shi, W.; Feng, J.; Li, Y. A comprehensive drought index based on remote sensing data and nested copulas for monitoring meteorological and agroecological droughts: A case study on the Qinghai-Tibet Plateau. *Environ. Model. Softw.* **2023**, *161*, 105629. [[CrossRef](#)]
29. Vicente-Serrano, S.M.; Beguería, S.; López-Moreno, J.I. A Multiscalar Drought Index Sensitive to Global Warming: The Standardized Precipitation Evapotranspiration Index. *J. Clim.* **2010**, *23*, 1696–1718. [[CrossRef](#)]
30. Li, R.; Chen, N.; Zhang, X.; Zeng, L.; Wang, X.; Tang, S.; Li, D.; Niyogi, D. Quantitative analysis of agricultural drought propagation process in the Yangtze River Basin by using cross wavelet analysis and spatial autocorrelation. *Agric. For. Meteorol.* **2020**, *280*, 107809. [[CrossRef](#)]
31. Sun, P.; Ma, Z.; Zhang, Q.; Singh, V.P.; Xu, C.-Y. Modified drought severity index: Model improvement and its application in drought monitoring in China. *J. Hydrol.* **2022**, *612*, 128097. [[CrossRef](#)]
32. Xu, H.; Zhu, Y.; Yagci, A.L.; Lü, H.; Gou, Q.; Wang, X.; Liu, E.; Ding, Z.; Pan, Y.; Liu, D.; et al. Development of composite drought indices for the coastal areas of southeastern China: A case study of Jinjiang and Jiulongjiang River basins. *J. Hydrol.* **2023**, *626*, 130210. [[CrossRef](#)]
33. Wang, Z.; Yang, Y.; Zhang, C.; Guo, H.; Hou, Y. Historical and future Palmer Drought Severity Index with improved hydrological modeling. *J. Hydrol.* **2022**, *610*, 127941. [[CrossRef](#)]
34. Liu, W.; Zhang, Y. Spatiotemporal Changes of sc-PDSI and Its Dynamic Drivers in Yellow River Basin. *Atmosphere* **2022**, *13*, 399. [[CrossRef](#)]
35. Han, X.; Wu, J.; Zhou, H.; Liu, L.; Yang, J.; Shen, Q.; Wu, J. Intensification of historical drought over China based on a multi-model drought index. *Int. J. Clim.* **2020**, *40*, 5407–5419. [[CrossRef](#)]
36. Lu, H.; Mo, X.; Liu, S. Intercomparison of three indices for addressing drought variability in North China Plain during 1962–2012. *Proc. Int. Assoc. Hydrol. Sci.* **2015**, *366*, 141–142. [[CrossRef](#)]
37. Huang, W.; Yang, J.; Liu, Y.; Yu, E. Spatiotemporal Variations of Drought in the Arid Region of Northwestern China during 1950–2012. *Adv. Meteorol.* **2021**, *2021*, 6680067. [[CrossRef](#)]
38. Zhao, H.; Gao, G.; An, W.; Zou, X.; Li, H.; Hou, M. Timescale differences between SC-PDSI and SPEI for drought monitoring in China. *Phys. Chem. Earth Parts A/B/C* **2017**, *102*, 48–58. [[CrossRef](#)]
39. Yu, H.; Zhang, Q.; Xu, C.-Y.; Du, J.; Sun, P.; Hu, P. Modified Palmer Drought Severity Index: Model improvement and application. *Environ. Int.* **2019**, *130*, 104951. [[CrossRef](#)] [[PubMed](#)]
40. Zhang, Y.; Li, G.; Ge, J.; Li, Y.; Yu, Z.; Niu, H. sc_PDSI is more sensitive to precipitation than to reference evapotranspiration in China during the time period 1951–2015. *Ecol. Indic.* **2018**, *96*, 448–457. [[CrossRef](#)]
41. Serkendiz, H.; Tatli, H.; Kılıç, A.; Çetin, M.; Sungur, A. Analysis of drought intensity, frequency and trends using the spei in Turkey. *Theor. Appl. Clim.* **2023**, *155*, 2997–3012. [[CrossRef](#)]
42. Stefanidis, S.; Rossiou, D.; Proutsos, N. Drought Severity and Trends in a Mediterranean Oak Forest. *Hydrology* **2023**, *10*, 167. [[CrossRef](#)]
43. Jin, N.; Shi, Y.; Niu, W.; He, L. Spatial and temporal patterns of agricultural drought in China during 1960–2020 characterized by use of the crop water deficit Abnormal Index. *J. Hydrol.* **2023**, *627*, 130454. [[CrossRef](#)]
44. Sun, H.; Di, Z.; Qin, P.; Zhang, S.; Lang, Y. Spatio-temporal variation and dynamic risk assessment of drought and flood disaster (DFD) in China. *Int. J. Disaster Risk Reduct.* **2024**, *100*, 104140. [[CrossRef](#)]
45. Huo, P.; Li, Z.; Bai, M.; Li, Z.; Huang, J.; Han, L. Spatial-temporal evolutions of historical and future meteorological drought center in Beijing area, China. *Urban Clim.* **2024**, *53*, 101786. [[CrossRef](#)]
46. Xue, Z.; Chen, Y.; Yin, Y.; Chen, W.; Jiao, Y.; Deng, P.; Dai, S. Spatio-temporal characteristics and driving factors of flash drought in northern China from 1978 to 2020. *Glob. Planet. Change* **2024**, *232*, 104326. [[CrossRef](#)]
47. Wang, H.; Gao, X.; Xu, T.; Xue, H.; He, W. Spatial-temporal evolution mechanism and efficiency evaluation of drought resilience system in China. *J. Clean. Prod.* **2023**, *428*, 139298. [[CrossRef](#)]
48. Zhang, J.-L.; Huang, X.-M.; Sun, Y.-Z. Multiscale spatiotemporal meteorological drought prediction: A deep learning approach. *Adv. Clim. Change Res.* **2024**, *15*, 211–221. [[CrossRef](#)]
49. Zhang, B.; Abu Salem, F.K.; Hayes, M.J.; Smith, K.H.; Tadesse, T.; Wardlow, B.D. Explainable machine learning for the prediction and assessment of complex drought impacts. *Sci. Total Environ.* **2023**, *898*, 165509. [[CrossRef](#)] [[PubMed](#)]
50. Yang, Y.; Li, K.; Wei, S.; Guga, S.; Zhang, J.; Wang, C. Spatial-temporal distribution characteristics and hazard assessment of millet drought disaster in Northern China under climate change. *Agric. Water Manag.* **2022**, *272*, 107849. [[CrossRef](#)]
51. Eini, M.R.; Salmani, H.; Piniewski, M. Comparison of process-based and statistical approaches for simulation and projections of rainfed crop yields. *Agric. Water Manag.* **2023**, *277*, 108107. [[CrossRef](#)]
52. Prodhon, F.A.; Zhang, J.; Sharma, T.P.P.; Nanzad, L.; Zhang, D.; Seka, A.M.; Ahmed, N.; Hasan, S.S.; Hoque, M.Z.; Mohana, H.P. Projection of future drought and its impact on simulated crop yield over South Asia using ensemble machine learning approach. *Sci. Total Environ.* **2022**, *807*, 151029. [[CrossRef](#)]

53. Dahal, N.M.; Xiong, D.; Neupane, N.; Yuan, Y.; Zhang, B.; Zhang, S.; Fang, Y.; Zhao, W.; Wu, Y.; Deng, W. Spatiotemporal assessment of drought and its impacts on crop yield in the Koshi River Basin, Nepal. *Theor. Appl. Clim.* **2023**, *155*, 1679–1698. [[CrossRef](#)]
54. Chou, J.; Jin, H.; Xu, Y.; Zhao, W.; Li, Y.; Hao, Y. Impacts and Risk Assessments of Climate Change for the Yields of the Major Grain Crops in China, Japan, and Korea. *Foods* **2024**, *13*, 966. [[CrossRef](#)]
55. Rezaei, E.E.; Webber, H.; Asseng, S.; Boote, K.; Durand, J.L.; Ewert, F.; Martre, P.; MacCarthy, D.S. Climate change impacts on crop yields. *Nat. Rev. Earth Environ.* **2023**, *4*, 831–846. [[CrossRef](#)]
56. China Meteorological Administration (CMA). *Handbook of Meteorological Geographical Regionalization in China*; Meteorological Press: Beijing, China, 2006.
57. Palmer, W.C. *Meteorological Drought*; Research Paper No. 45; US Weather Bureau: Washington, DC, USA, 1965.
58. Shen, G.Q.; Zheng, H.F.; Lei, Z.F. Spatiotemporal analysis of meteorological drought (1961–2014) in Northeast China using a standardized precipitation evapotranspiration index. *Act Ecol. Sin.* **2017**, *37*, 5882–5893.
59. Zhao, Y.; Zheng, R.; Zheng, F.; Zhong, K.; Fu, J.; Zhang, J.; Flanagan, D.C.; Xu, X.; Li, Z. Spatiotemporal distribution of agrometeorological disasters in China and its impact on grain yield under climate change. *Int. J. Disaster Risk Reduct.* **2023**, *95*, 103823. [[CrossRef](#)]
60. Zhu, X.; Liu, T.; Xu, K.; Chen, C. The impact of high temperature and drought stress on the yield of major staple crops in northern China. *J. Environ. Manag.* **2022**, *314*, 115092. [[CrossRef](#)] [[PubMed](#)]
61. Yu, L.; Zhao, X.; Gao, X.; Jia, R.; Yang, M.; Yang, X.; Wu, Y.; Siddique, K.H. Effect of natural factors and management practices on agricultural water use efficiency under drought: A meta-analysis of global drylands. *J. Hydrol.* **2021**, *594*, 125977. [[CrossRef](#)]
62. Feng, S.; Hao, Z.; Zhang, X.; Hao, F. Probabilistic evaluation of the impact of compound dry-hot events on global maize yields. *Sci. Total Environ.* **2019**, *689*, 1228–1234. [[CrossRef](#)]
63. Feng, S.; Hao, Z. Quantifying likelihoods of extreme occurrences causing maize yield reduction at the global scale. *Sci. Total Environ.* **2020**, *704*, 135250. [[CrossRef](#)]
64. Guo, S.M.; Ma, S.; Chen, Y.J. The Situation and comparative advantage and problems and countermeasures of grain product of the three provinces in east–north areas. *Chin. Agric. Sci.* **2006**, *22*, 488–493. (In Chinese)
65. Chen, C.; Lei, C.; Deng, A.; Qian, C.; HooDMoed, W.; Zhang, W. Will higher minimum temperatures increase corn production in Northeast China? An analysis of historical data over 1965–2008. *Agric. For. Meteorol.* **2011**, *151*, 1580–1588. [[CrossRef](#)]
66. Wang, S.; Huang, X.; Zhang, Y.; Yin, C.; Richel, A. The effect of corn straw return on corn production in Northeast China: An integrated regional evaluation with meta-analysis and system dynamics. *Resour. Conserv. Recycl.* **2021**, *167*, 105402. [[CrossRef](#)]
67. Wan, W.; Liu, Z.; Li, K.; Wang, G.; Wu, H.; Wang, Q. Drought monitoring of the maize planting areas in Northeast and North China Plain. *Agric. Water Manag.* **2021**, *245*, 106636. [[CrossRef](#)]
68. Wan, W.; Liu, Z.; Li, J.; Xu, J.; Wu, H.; Xu, Z. Spatiotemporal patterns of maize drought stress and their effects on biomass in the Northeast and North China Plain from 2000 to 2019. *Agric. For. Meteorol.* **2022**, *315*, 108821. [[CrossRef](#)]
69. Liu, S.; Xiao, L.; Sun, J.; Yang, P.; Yang, X.; Wu, W. Probability of maize yield failure increases with drought occurrence but partially depends on local conditions in China. *Eur. J. Agron.* **2022**, *139*, 126552. [[CrossRef](#)]
70. Guo, E.; Liu, X.; Zhang, J.; Wang, Y.; Wang, C.; Wang, R.; Li, D. Assessing spatiotemporal variation of drought and its impact on maize yield in Northeast China. *J. Hydrol.* **2017**, *553*, 231–247. [[CrossRef](#)]
71. Zhou, Z.; Shi, H.; Fu, Q.; Li, T.; Gan, T.Y.; Liu, S. Assessing spatiotemporal characteristics of drought and its effects on climate-induced yield of maize in Northeast China. *J. Hydrol.* **2020**, *588*, 125097. [[CrossRef](#)]
72. Liu, S.; Wu, W.; Yang, X.; Yang, P.; Sun, J. Exploring drought dynamics and its impacts on maize yield in the Huang-Huai-Hai farming region of China. *Clim. Change* **2020**, *163*, 415–430. [[CrossRef](#)]
73. Huanhe, W.; Xiaoyu, G.; Xiang, Z.; Wang, Z.; Xubin, Z.; Yinglong, C.; Zhongyang, H.; Guisheng, Z.; Tianyao, M.; Qigen, D. Grain Yield, Biomass Accumulation, and Leaf Photosynthetic Characteristics of Rice under Combined Salinity-Drought Stress. *Rice Sci.* **2024**, *31*, 118–128. [[CrossRef](#)]
74. Shailani, A.; Joshi, R.; Singla-Pareek, S.L.; Pareek, A. Stacking for future: Pyramiding genes to improve drought and salinity tolerance in rice. *Physiol. Plant.* **2020**, *172*, 1352–1362. [[CrossRef](#)]
75. Latif, A.; Ying, S.; Cuixia, P.; Ali, N. Rice Curled Its Leaves Either Adaxially or Abaxially to Combat Drought Stress. *Rice Sci.* **2023**, *30*, 405–416. [[CrossRef](#)]
76. Zhan, C.; Liang, C.; Zhao, L.; Jiang, S.; Zhang, Y. Differential responses of crop yields to multi-timescale drought in mainland China: Spatiotemporal patterns and climate drivers. *Sci. Total Environ.* **2024**, *906*, 167559. [[CrossRef](#)] [[PubMed](#)]
77. Chengqi, Z.; Yuxuan, Y.; Tian, Q.; Yafan, H.; Jifeng, Y.; Zhicheng, S. Drought-Tolerant Rice at Molecular Breeding Eras: An Emerging Reality. *Rice Sci.* **2024**, *31*, 179–189. [[CrossRef](#)]
78. Liu, Y.; Chen, Q.; Chen, J.; Pan, T.; Ge, Q. Plausible changes in wheat-growing periods and grain yield in China triggered by future climate change under multiple scenarios and periods. *Q. J. R. Meteorol. Soc.* **2021**, *147*, 4371–4387. [[CrossRef](#)]
79. Helman, D.; Bonfil, D.J. Six decades of warming and drought in the world’s top wheat-producing countries offset the benefits of rising CO₂ to yield. *Sci. Rep.* **2022**, *12*, 7921. [[CrossRef](#)] [[PubMed](#)]
80. Ye, J.; Gao, Z.; Wu, X.; Lu, Z.; Li, C.; Wang, X.; Chen, L.; Cui, G.; Yu, M.; Yan, G.; et al. Impact of increased temperature on spring wheat yield in northern China. *Food Energy Secur.* **2021**, *10*, 368–378. [[CrossRef](#)]

81. Geng, G.; Yang, R.; Chen, Q.; Deng, T.; Yue, M.; Zhang, B.; Gu, Q. Tracking the influence of drought events on winter wheat using long-term gross primary production and yield in the Wei River Basin, China. *Agric. Water Manag.* **2023**, *275*, 108019. [[CrossRef](#)]
82. Wang, J.; Fang, F.; Wang, J.; Yue, P.; Wang, S.; Xu, Y. Evolutionary characteristics and influencing factors of wheat production risk in Gansu Province of China under the background of climate change. *Theor. Appl. Clim.* **2024**, 1–27. [[CrossRef](#)]
83. Wang, F.; Fu, B.; Liang, W.; Jin, Z.; Zhang, L.; Yan, J.; Fu, S.; Gou, F. Assessment of drought and its impact on winter wheat yield in the Chinese Loess Plateau. *J. Arid Land* **2022**, *14*, 771–786. [[CrossRef](#)]
84. Zhang, L.; Chu, Q.-Q.; Jiang, Y.-L.; Chen, F.; Lei, Y.-D. Impacts of climate change on drought risk of winter wheat in the North China Plain. *J. Integr. Agric.* **2021**, *20*, 2601–2612. [[CrossRef](#)]
85. Wu, J.; Gu, Y.; Sun, K.; Wang, N.; Shen, H.; Wang, Y.; Ma, X. Correlation of climate change and human activities with agricultural drought and its impact on the net primary production of winter wheat. *J. Hydrol.* **2023**, *620*, 129504. [[CrossRef](#)]
86. Mills, G.; Sharps, K.; Simpson, D.; Pleijel, H.; Broberg, M.; Uddling, J.; Jaramillo, F.; Davies, W.J.; Dentener, F.; Berg, M.V.D.; et al. Ozone pollution will compromise efforts to increase global wheat production. *Glob. Change Biol.* **2018**, *24*, 3560–3574. [[CrossRef](#)] [[PubMed](#)]

Disclaimer/Publisher’s Note: The statements, opinions and data contained in all publications are solely those of the individual author(s) and contributor(s) and not of MDPI and/or the editor(s). MDPI and/or the editor(s) disclaim responsibility for any injury to people or property resulting from any ideas, methods, instructions or products referred to in the content.